International Journal of Microscale and Nanoscale Thermal … ISSN: 1949-4955
Volume 5, Issue 1

FLOW AND HEAT TRANSFER OF TWO MICROPOLAR FLUIDS SEPARATED BY A VISCOUS FLUID LAYER

J. C. Umavathi[1], Ali J. Chamkha[2*] and M. Shekar[1]

[1]Department of Mathematics, Gulbarga University, Gulbarga, Karnataka, India
[2]Manufacturing Engineering Department,
The Public Authority for Applied Education and Training, Shuweikh, Kuwait

ABSTRACT

An analysis of the viscous fluid sandwiched between micropolar fluids is presented. The channel walls are maintained at two different constant temperatures. The transport properties of the fluids in all regions are assumed to be constant. Exact analytical solutions are found by integrating the governing equations and also by using semi-numerical-analytical method called Differential Transform Method. The solutions are also evaluated numerically and shown graphically for various governing parameters on velocity, microrotation velocity and temperature profiles. The variation of the rate of heat transfer, skin friction and mass flow rate for different values of viscosity ratio $(0.5 \le m \le 2.0)$, conductivity ratio $(0.1 \le Cr \le 2.0)$, material parameter $(0 \le K \le 2)$, Eckert number $(0.1 \le Ec \le 2.0)$, and Prandtl number $(0.1 \le \Pr \le 2.0)$ are presented in tabular form. It is found that the rate of heat transfer decreases at the top plate and increases at the bottom plate for variations of viscosity ratio, material parameter, conductivity ratio, Eckert number and Prandtl number. The mass flow rate decreases as the viscosity ratio and material parameter increases whereas it is not affected for variations of conductivity ratio, Eckert number and Prandtl number.

Keywords: Micropolar fluid, Differential Transform method, heat transfer

NOMENCLATURE

Cr	conductivity ratio $[K_1/K_C]$
Ec	Eckert number
h	height of the channel $[\mathrm{m}]$
j_d	microinertia density $[\mathrm{m}^2]$

* Corresponding author. E-mail address: achamkha@yahoo.com (A.J. Chamkha).

K	material parameter
K_1	thermal conductivity of the micropolar fluid $\left[\mathrm{Wm^{-1}K^{-1}}\right]$
K_C	thermal conductivity of the viscous fluid $\left[\mathrm{Wm^{-1}K^{-1}}\right]$
m	viscosity ratio $\left[\mu_1/\mu\right]$
M	mass flow rate
$N_{1,3}$	microrotation velocity
P	pressure gradient $\left[\mathrm{Nm^{-2}}\right]$
Pr	Prandtl number
q	rate of heat transfer
T_{W1}, T_{W2}	wall temperatures $\left[\mathrm{K}\right]$
T_i	temperature $\left[\mathrm{K}\right]$
U_i	velocity $\left[\mathrm{ms^{-1}}\right]$
u_i	dimensionless velocity
$\bar{u}_1$	average velocity $\left[\mathrm{ms^{-1}}\right]$
$\left(X,Y\right)$	space coordinate $\left[\mathrm{m}\right]$

Greek Symbols

μ	viscosity of the micropolar fluid $\left[\mathrm{kg\,m^{-1}s^{-1}}\right]$
μ_1	viscosity of the viscous fluid $\left[\mathrm{kg\,m^{-1}s^{-1}}\right]$
κ	vortex viscosity
γ	spin-gradient viscosity $\left[\mathrm{kg\,m^{-1}s^{-1}}\right]$
θ_i	dimensionless temperature
τ	skin friction

Subscripts

B	bottom wall
T	top wall
$i=1,2,3$	refers the region-I, region-II and region-III respectively
$j=1,3$	refers the region-I, and region-III respectively

1. INTRODUCTION

The Navier–Stokes model of classical hydrodynamics is inadequate to describe some modern engineering structures which are often made up of materials possessing an internal structure. Polycrystalline materials, fluids containing additives and the materials with fibrous or coarse grain structure fall in this category. The presence of a small amount of additives in the fluid significantly lower down the skin friction near a rigid body and also the frictional drag is reduced by polymer concentration [1]. The classical continua fail to accurately predict the physical nature of asymmetric deformation of these materials. The theory of micropolar fluids introduced by Eringen [2, 3] is one of the best theories of fluids to describe the deformation of such materials. Polymeric suspensions, biological fluids, liquid crystals with rigid molecules, muddy fluids, and nemotogenic and smectogenic liquid crystals are some examples of such fluids. Physically these fluids may represent the fluids consisting of rigid randomly oriented particles suspended in a viscous medium undergoing both translational and rotational motion. These fluids can support stress moments and body couples and is influenced by the spin inertia. The stress tensor is not symmetric for such fluid. Micropolar fluids are those which contain micro-constituents that can undergo rotation, the presence of which can affect the hydrodynamics of the flow so that it can be distinctly non-Newtonian. It has many practical applications, for example, analyzing the behavior of exotic lubricants ([4] and [5]), the flow of colloidal suspensions or polymeric fluids [6], liquid crystals ([7] and [8]), additive suspensions, human and animal blood [9], turbulent shear flow and so forth. Extensive reviews of the theory and applications can be found in the review articles by Ariman et al. [9, 10] and the books by Lukaszewicz [11] and Eringen [12]. Umavathi and Sultana [13] analyzed the analytical solutions of fully-developed mixed convection for the laminar flow of a micropolar fluid in a parallel plate vertical channel with heat source/sink. Rashidi et al. [14] found the complete analytic solution to heat transfer of a micropolar fluid through a porous medium with radiation using Homotopy analysis method. Most recently, Ziaul Haque et al. [15] studied numerical behavior of micropolar fluid on steady MHD free convection and mass transfer through a porous medium with constant heat and mass fluxes.

Along with the advancement of science and technology, there is an increased need for conserving useful energy and thus, producing thermodynamically efficient heat transfer processes in which internal forced convection heat transfer occurs. The flow and heat transfer aspects of immiscible fluids are of special importance in the petroleum extraction and transport problem since the reservoir rock of an oil field always contains several immiscible fluids in its pores. Part of the pore volume is occupied by water and the rest may be occupied either by oil or gas or both. Crude oils often contain dissolved gases which may be released into the reservoir rock when the pressure decreases. In modeling such problems, the presence of a second immiscible fluid phase adds number of complexities as to the nature of interacting transport phenomena and interface conditions between phases. On the other hand, the only flows of two immiscible fluids are also important problem in engineering applications for both Newtonian–Newtonian and Newtonian–non-Newtonian fluids. Especially in crude oil transportation and designing of lubricated pipelines the wax problem can be prevented with well design.

Bakhtiyarov and Siginer [16] made an experiment to investigate the flow behavior of two immiscible non-Newtonian and Newtonian fluids in a tube using an opto-mechanical method to solve the crude oil transportation problems. Chamkha [17] performed an analytical study by using two-term harmonic and non-harmonic functions to investigate the oscillatory flow and heat transfer for two viscous immiscible fluids through a horizontal channel with permeable walls. Their results are presented for different Prandtl number, viscosity ratio and conductivity ratio. Chamkha [18] investigated the flow fields of two-immiscible viscous, incompressible, electrically conducting and heat-generating or absorbing fluids in porous medium and the governing equations were solved numerically. He reported that flow can be controlled by considering different fluids having viscosities, conductivities and oscillation amplitude. Umavathi et al. [19] found the closed-form solutions for steady laminar fully developed flow and heat transfer in a horizontal channel consisting of a couple-stress fluid sandwiched between two clear viscous fluids. Umavathi et al. [20] also presented the model for blood flow through a horizontal channel. The model essentially consists of a core region assumed to be a micropolar fluid and two viscous (Newtonian) fluid regions. It was observed that the material parameter and viscosity ratio affect the position of the point of flow separation for which the flow nature is reversed. Ikbal et al. [21] analyzed the unsteady two-layered blood flow through a flexible artery under stenotic conditions where the flowing blood was represented by the two-fluid model, consisting of a core region of suspension of all erythrocytes assumed to be Eringen's micropolar fluid and a plasma layer free from cells of any kind as a Newtonian fluid. Umavathi et al. [22-25] and Malashetty et al. [26, 27] analyzed the flow and heat transfer characteristics of immiscible fluids in different geometries. Recently, Prathap Kumar et al. [28] studied analytically fully-developed laminar free-convection flow in a vertical channel with one region filled with micropolar fluid and the other region with a viscous fluid.

One of the semi-numerical-exact methods which do not need small parameters is the Differential Transform Method (DTM). This method was first proposed by Zhou [29], who solved linear and nonlinear problems in electrical circuits. Chen and Ho [30] developed this method for partial differential equations and Ayaz [31] applied it to the system of differential equations; and this method is very powerful [32]. This method constructs an analytical solution in the form of a polynomial. It is different from the traditional higher-order Taylor series method. The Taylor series method is computationally expensive for large orders. The differential transform method is an alternative procedure for obtaining an analytic Taylor series solution of differential equations. In recent years, the differential transform method has been successfully employed to solve many types of nonlinear problems [33–40].

The main goal of the present study is to find a totally analytic solution for heat transfer of a viscous fluid sandwiched between micropolar fluids in horizontal channel by the differential transform method and by direct method. The convergence of the obtained series solutions is carefully analyzed. It is found that the results obtained by DTM agree very well with the direct method (exact solutions).

2. Mathematical Formulation

The physical configuration (Figure 1) consists of three infinite, horizontal parallel plates extending in the X and Y directions. The flow and heat transfer in a system consists of a viscous fluid layer sandwiched between two micropolar fluid layers. The region $-h \le Y \le 0$ and $h \le Y \le 2h$ is filled with a micropolar fluid of viscosity μ_1, vortex viscosity κ, thermal conductivity K_1 and the region $0 \le Y \le h$ is occupied by a viscous fluid having a viscosity μ, thermal conductivity K_C. The boundary walls of the channel are held at different constant temperatures T_{W1} and the lower wall is held at a temperature T_{W2} with $T_{W1} > T_{W2}$. The flow is assumed to be steady, laminar and fully developed. Further, the fluid in all regions is assumed to be driven by a common constant pressure gradient $\left(-\partial p/\partial X\right)$ and the existence of heat transfer does not affect the pressure gradient. The transport properties of the fluids in all regions are assumed to be constant.

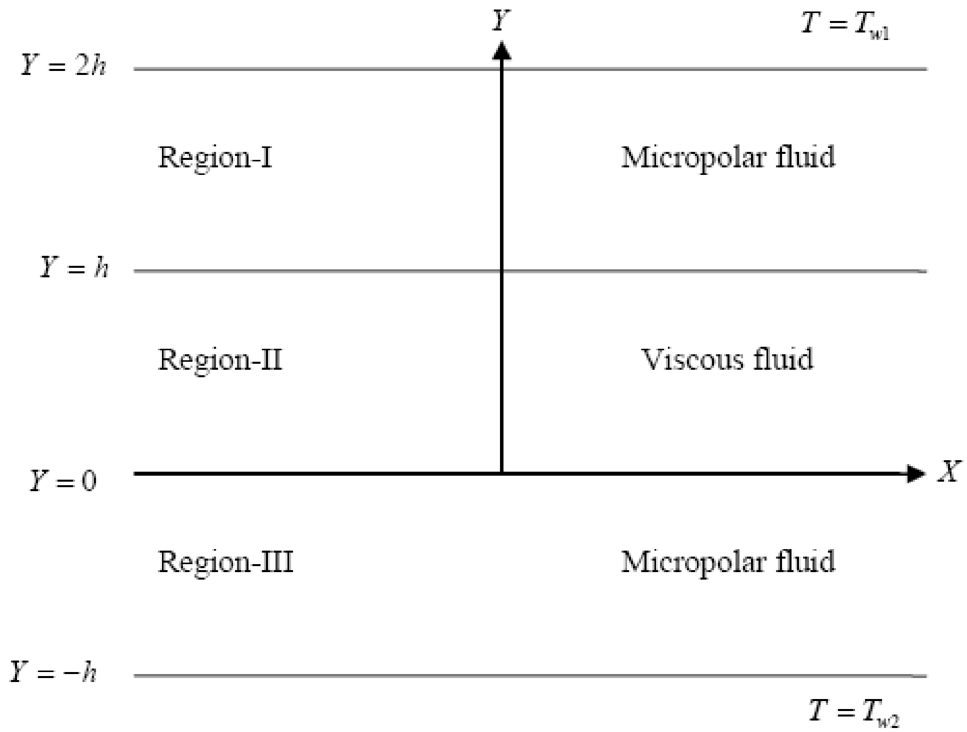

Figure 1. Physical configuration and coordinate system.

Under these assumptions, the governing equations of motion, microrotation and energy are (Chamkha [18]):

Region-1:

$$\left(\mu_1 + \kappa\right)\frac{d^2U_1}{dY^2} + \kappa\frac{dN_1}{dY} - \frac{\partial p}{\partial X} = 0 \tag{1}$$

$$\gamma\frac{d^2N_1}{dY^2} - 2\kappa N_1 - \kappa\frac{dU_1}{dY} = 0 \tag{2}$$

$$K_1\frac{d^2T_1}{dY^2} + \mu_1\left(\frac{dU_1}{dY}\right)^2 = 0 \tag{3}$$

for $h \le Y \le 2h$,

Region-2:

$$\mu \frac{d^2U_2}{dY^2} - \frac{\partial p}{\partial X} = 0 \tag{4}$$

$$K_C \frac{d^2T_2}{dY^2} + \mu\left(\frac{dU_2}{dY}\right)^2 = 0 \tag{5}$$

for $0 \le Y \le h$,

Region-3:

$$(\mu_1 + \kappa)\frac{d^2U_3}{dY^2} + \kappa\frac{dN_3}{dY} - \frac{\partial p}{\partial X} = 0 \tag{6}$$

$$\gamma \frac{d^2N_3}{dY^2} - 2\kappa N_3 - \kappa\frac{dU_3}{dY} = 0 \tag{7}$$

$$K_1 \frac{d^2T_3}{dY^2} + \mu_1\left(\frac{dU_3}{dY}\right)^2 = 0 \tag{8}$$

for $-h \le Y \le 0$

where U_i $(i = 1, 2, 3)$ is the X-component of the fluid velocity in the three regions, T_i $(i = 1, 2, 3)$ is the fluid temperature in the three regions, $N_{1,3}$ is the component of microrotation vector normal to the plane (X,Y) and γ is the spin-gradient viscosity. Further, it is assumed that γ has the following form as proposed by Rees and Basoom [41].

$$\gamma = \left(\mu_1 + \frac{\kappa}{2}\right) j_d = \mu_1\left(1 + \frac{K}{2}\right) j_d$$

where $K = \kappa/\mu_1$ is called the material parameter and j_d is the microinertia density.

To solve the above system of Eqs. (1)–(8) ten boundary conditionns are required for velocity and six boundary conditions for temperature. The first two boundary conditions are obtained from the fact that there is no slip near the wall. Next two conditions are obtained by assuming the continuity of velocity and the last six conditions are obtained from the equality of stresses at the interface and constant cell rotational velocity at the interface as proposed by Ariman et al. [9]. Thus, the appropriate boundary and interface conditions on velocity in the mathematical form are

$$U_3 = 0 \quad \text{at} \quad Y = -h\,,\ U_1 = 0 \quad \text{at} \quad Y = 2h$$
$$U_1(h) = U_2(h)\,,\ U_2(0) = U_3(0)$$
$$\left(\mu_1 + \kappa\right)\frac{dU_1}{dY} + \kappa N_1 = \mu\frac{dU_2}{dY} \ \text{ at } Y = h$$
$$\mu\frac{dU_2}{dY} = \left(\mu_1 + \kappa\right)\frac{dU_3}{dY} + \kappa N_3 \ \text{ at } Y = 0$$
$$\frac{dN_1}{dY} = 0 \ \text{ at } Y = h\,,\ \frac{dN_3}{dY} = 0 \ \text{ at } Y = 0$$
$$N_3 = 0 \ \text{ at } Y = -h\,,\ N_1 = 0 \ \text{ at } Y = 2h \qquad (9)$$

The six boundary and interface conditions on the temperature are as follows: the upper wall is held at a temperatures T_{W1} and the lower wall is held at a temperature T_{W2} with $T_{W1} > T_{W2}$. The other four conditions are the continuity of temperature and heat flux at the two interfaces.

$$T_3 = T_{W2} \ \text{ at } \quad Y = -h\,,\ T_1 = T_{W1} \ \text{ at } \quad Y = 2h$$
$$T_1(h) = T_2(h)\,,\ T_2(0) = T_3(0)$$
$$K_C\frac{dT_2}{dY} = K_1\frac{dT_3}{dY} \ \text{ at } Y = 0\,, K_1\frac{dT_1}{dY} = K_C\frac{dT_2}{dY} \ \text{ at } Y = h \qquad (10)$$

Equations (1) – (10) are made dimensionless by using the following dimensionless flow variables

$$u_i = \frac{U_i}{\bar{u}_1}\,,\ y = \frac{Y}{h}\,,\ \theta_i = \frac{T_i - T_{w2}}{T_{W1} - T_{w2}}\,,\ N_i^* = \frac{h}{\bar{u}_1}N_i\,,\ K = \frac{\kappa}{\mu_1}\,,\ j_d = h^2\,,\ Ec = \frac{\bar{u}_1^{\,2}}{C_p\left(T_{w1} - T_{w2}\right)}\,,$$
$$\Pr = \frac{C_p\mu}{K_1}\,,\ Cr = \frac{K_1}{K_C}\,,\ m = \frac{\mu_1}{\mu}\,,\ P = \frac{h^2}{\mu_1\bar{u}_1^{\,2}}\frac{\partial p}{\partial X} \qquad (11)$$

where $\bar{u}_1$ is the average velocity, m is the viscosity ratio, Cr is the conductivity ratio, P is the pressure gradient, Ec is the Eckert number and $\Pr$ is the Prandtl number.

Using Eq. (11), Eqs. (1) – (10) yield, after dropping the asterisk, the following equations in the three regions:

Region 1:

$$\left(1 + K\right)\frac{d^2u_1}{dy^2} + K\frac{dN_1}{dy} = P \qquad (12)$$
$$\left(1 + \frac{K}{2}\right)\frac{d^2N_1}{dy^2} - 2KN_1 - K\frac{du_1}{dy} = 0 \qquad (13)$$

$$\frac{d^2\theta_1}{dy^2}+Ec\Pr\left(\frac{du_1}{dy}\right)^2=0 \tag{14}$$

Region-2:

$$\frac{d^2u_2}{dy^2}=mP \tag{15}$$

$$\frac{d^2\theta_2}{dy^2}+\frac{Ec\Pr Cr}{m}\left(\frac{du_2}{dy}\right)^2=0 \tag{16}$$

Region-3:

$$\left(1+K\right)\frac{d^2u_3}{dy^2}+K\frac{dN_3}{dy}=P \tag{17}$$

$$\left(1+\frac{K}{2}\right)\frac{d^2N_3}{dy^2}-2KN_3-K\frac{du_3}{dy}=0 \tag{18}$$

$$\frac{d^2\theta_3}{dy^2}+Ec\Pr\left(\frac{du_3}{dy}\right)^2=0 \tag{19}$$

The non-dimensional form of the velocity and microrotation velocity boundary and interface conditions become

$$\begin{gathered}
u_3=0 \quad \text{at} \quad y=-1,\ u_1=0 \quad \text{at} \quad y=2\\
u_2\left(0\right)=u_3\left(0\right),\ u_1\left(1\right)=u_2\left(1\right)\\
\frac{1}{m}\frac{du_2}{dy}=\left(1+K\right)\frac{du_3}{dy}+KN_3 \ \text{ at } \ y=0\\
\left(1+K\right)\frac{du_1}{dy}+KN_1=\frac{1}{m}\frac{du_2}{dy} \ \text{ at } \ y=1
\end{gathered} \tag{20}$$

$$\frac{dN_3}{dy}=0 \ \text{ at } \ y=0,\ \frac{dN_1}{dy}=0 \ \text{ at } \ y=1$$

$$N_3=0 \ \text{ at } \ y=-1,\ N_1=0 \ \text{ at } \ y=2$$

The non-dimensional form of the temperature boundary and interface conditions become

$$\theta_3=0 \quad \text{at} \quad y=-1,\ \theta_1=1 \quad \text{at} \quad y=2$$

$$\theta_2(0)=\theta_3(0),\ \theta_1(1)=\theta_2(1)$$

$$\frac{d\theta_2}{dy} = Cr\frac{d\theta_3}{dy} \text{ at } y=0\,,\ \frac{d\theta_1}{dy} = \frac{1}{Cr}\frac{d\theta_2}{dy} \text{ at } y=1 \tag{21}$$

3. SOLUTIONS

3.1. Closed-Form Solutions

The expressions for the non-dimensional velocityes u_i (i = 1, 2, 3), the microrotation velocity N_j (j = 1, 3), and the temperatures θ_i (i = 1, 2, 3) obtained as the solutions of (12)–(19) with boundary and interface conditions (20) and (21)are:

Region-1:

$$u_1 = D_3 y + D_4 + l_1\cosh(ay) + l_2\sinh(ay) + l_3 y^2 \tag{22}$$

$$\theta_1 = B_1\cosh(2ay) + B_2\sinh(2ay) + (B_3 y + B_5)\cosh(ay) + (B_4 y + B_6)\sinh(ay) + B_7 y^4 + B_8 y^3 + B_9 y^2 + C_1 y + C_2 \tag{23}$$

$$N_1 = D_1\cosh(ay) + D_2\sinh(ay) - \frac{Py}{K+2} - \left(\frac{K+1}{K+2}\right)A \tag{24}$$

Region-2:

$$u_2 = \frac{mP}{2}y^2 + D_5 y + D_6 \tag{25}$$

$$\theta_2 = C_3 y + C_4 + B_{10} y^4 + B_{11} y^3 + B_{12} y^2 \tag{26}$$

Region-3:

$$u_3 = D_9 y + D_{10} + l_4\cosh(ay) + l_5\sinh(ay) + l_3 y^2 \tag{27}$$

$$\theta_3 = (B_{15} y + B_{17})\cosh(ay) + (B_{16} y + B_{18})\sinh(ay) + B_{13}\cosh(2ay) + B_{14}\sinh(2ay) + B_{19} y^4 + B_{20} y^3 + B_{21} y^2 + C_5 y + C_6 \tag{28}$$

$$N_3 = D_7\cosh(ay) + D_8\sinh(ay) - \frac{Py}{K+2} - \left(\frac{K+1}{K+2}\right)B \tag{29}$$

where $a = \sqrt{\frac{2K}{K+1}}$, D_i's $(i = 1 \text{ to } 10)$, C_j's $(j = 1 \text{ to } 6)$, A and B are constants.

3.2. Differential Transform Method

The differential transformation of an analytical function $U(k)$ for one variable is defined as (Zhou [29])

$$U(r)=\frac{1}{r!}\left[\frac{d^r u(y)}{dy^r}\right]_{y=0}, \tag{30}$$

and the inverse differential transformation is given by

$$u(y)=\sum_{r=0}^{\infty}U(k)\,y^r , \tag{31}$$

Combining Eqs. (30) and (31), we obtain

$$u(y)=\sum_{r=0}^{\infty}\frac{y^r}{r!}\frac{d^r u(y)}{dy^r}\bigg|_{y=0}, \tag{32}$$

From Eqs. (30)–(32), it can be seen that the differential transformation method is derived from Taylor's series expansion. In real applications $\sum_{r=n}^{\infty}U(k)\,y^r$ is very small and can be neglected when n is sufficiently large. So $u(y)$ can be expressed by a finite series, and Eq. (31) may be written as

$$u(y)=\sum_{r=0}^{n}U(k)\,y^r \tag{33}$$

where the value of n depends on the convergence requirement in real applications and $U(k)$ is the differential transform of $u(y)$. Table-1 lists the basic mathematical operations frequently used in the following analysis.

Taking differential transform of Eqs. (12)–(19), one can obtain the transformed equations as

Region-1:

$$(1+K)(r+1)(r+2)U_1[r+2]+K(r+1)H_1[r+1]=P\delta[r] \tag{34}$$

$$\left(1+\frac{K}{2}\right)(r+1)(r+2)H_1[r+2]-2KH_1[r]-K(r+1)U_1[r+1]=0 \tag{35}$$

$$\left(r+1\right)\left(r+2\right)\Theta_1\left[r+2\right]+Ec\Pr\sum_{s=0}^{r}\left(s+1\right)U_1\left[s+1\right]\left(r-s+1\right)U_1\left[r-s+1\right]=0 \tag{36}$$

Region-2:

$$\left(r+1\right)\left(r+2\right)U_1\left[r+2\right]=mP\delta\left[r\right] \tag{37}$$

$$\left(r+1\right)\left(r+2\right)\Theta_2\left[r+2\right]+\frac{Ec\Pr Cr}{m}\sum_{s=0}^{r}\left(s+1\right)U_2\left[s+1\right]\left(r-s+1\right)U_2\left[r-s+1\right]=0 \tag{38}$$

Region-3:

$$\left(1+K\right)\left(r+1\right)\left(r+2\right)U_3\left[r+2\right]+K\left(r+1\right)H_3\left[r+1\right]=P\delta\left[r\right] \tag{39}$$

$$\left(1+\frac{K}{2}\right)\left(r+1\right)\left(r+2\right)H_3\left[r+2\right]-2K\,H_3\left[r\right]-K\left(r+1\right)U_3\left[r+1\right]=0 \tag{40}$$

$$\left(r+1\right)\left(r+2\right)\Theta_3\left[r+2\right]+Ec\Pr\sum_{s=0}^{r}\left(s+1\right)U_3\left[s+1\right]\left(r-s+1\right)U_3\left[r-s+1\right]=0 \tag{41}$$

where, $U_i\left(k\right)$, $H_j\left(k\right)$ and $\Theta_i\left(k\right)$ are the transformed notations of $u_i\left(y\right)$, $N_j\left(y\right)$ and $\theta_i\left(\eta\right)$ ($i=1,2,3$, $j=1,3$) respectively.

Table 1. The operations for the one-dimensional differential transform method

Original function	Transformed function
$y(\eta)=g(\eta)\pm h(\eta)$	$Y(k)=G(k)\pm H(k)$
$y(\eta)=\alpha\, g(\eta)$	$Y(k)=\alpha\, G(k)$
$y(\eta)=\dfrac{dg(\eta)}{d\eta}$	$Y(k)=(k+1)G(k+1)$
$y(\eta)=\dfrac{d^2g(\eta)}{d\eta^2}$	$Y(k)=(k+1)(k+2)G(k+2)$
$y(\eta)=g(\eta)h(\eta)$	$Y(k)=\sum_{l=0}^{k}G(l)H(k-l)$
$y(\eta)=\eta^m$	$Y(k)=\delta(k-m)=\begin{cases}1, \text{ if } k=m\\ 0, \text{ if } k\neq m\end{cases}$

The differential transform for boundary value problems are indeterminate, thus we must consider the boundary conditions (20) and (21) as follows

$$u_1(0)=\alpha_1,\ \frac{du_1}{dy}(0)=\alpha_2,\ u_2(0)=u_3(0)=\alpha_3,\ \frac{du_3}{dy}(0)=\alpha_4,$$
$$\frac{du_2}{dy}(0)=m\left((1+K)\frac{du_3}{dy}(0)+KN_3(0)\right),$$
$$N_1(0)=\beta_1,\ \frac{dN_1}{dy}(0)=\beta_2,\ \frac{dN_3}{dy}(0)=0,\ N_3(0)=\beta_3,$$
$$\theta_1(0)=\gamma_1,\ \frac{d\theta_1}{dy}(0)=\gamma_2,\ \theta_2(0)=\theta_3(0)=\gamma_3,\ \frac{d\theta_2}{dy}(0)=\gamma_4,\ \frac{d\theta_3}{dy}(0)=\frac{1}{Cr}\frac{d\theta_2}{dy}(0) \tag{42}$$

where α_i, β_i and γ_i 's are unknowns.

Therefore the problem changes to an initial value problem. The differential transform of the boundary conditions are as follows

$$U_1[0]=\alpha_1,\ U_1[1]=\alpha_2,\ U_2[0]=U_3[0]=\alpha_3,\ U_3[1]=\alpha_4,\ U_2[1]=m\big((1+K)U_3[1]+KH_3[0]\big),$$
$$H_1[0]=\beta_1,\ H_1[1]=\beta_2,\ H_3[1]=0,\ H_3[0]=\beta_3,$$
$$\Theta_1[0]=\gamma_1,\ \Theta_1[1]=\gamma_2,\ \Theta_2[0]=\Theta_3[0]=\gamma_3,\ \Theta_2[1]=\gamma_4,\ \Theta_3[1]=\frac{\Theta_2[1]}{Cr}. \tag{43}$$

Moreover, substituting Eqs. (43) into Eqs. (34)–(41) and by recursive method we can calculate another value of $U_i[k],\ H_j[k],\ \Theta_i[k]\ \ (i=1,2,3,\ j=1,3)$. Hence, substituting all $U_i[k],\ H_j[k],\ \Theta_i[k]$ into Eq. (33), the series solutions are obtained. After finding the series solutions, the unknowns are evaluated using Eqs. (20) and (21).

Further, we shall consider some particular cases of the problem under consideration.

Case-1: Newtonian Fluid $(K=0)$

For a Newtonian fluid $(K=0)$, the non-dimensional basic equations become

Region 1:

$$\frac{d^2u_1}{dy^2}=P \tag{44}$$

$$\frac{d^2\theta_1}{dy^2}+Ec\Pr\left(\frac{du_1}{dy}\right)^2=0 \tag{45}$$

Region-2:

$$\frac{d^2u_2}{dy^2}=mP \tag{46}$$

$$\frac{d^2\theta_2}{dy^2} + \frac{Ec\,\Pr Cr}{m}\left(\frac{du_2}{dy}\right)^2 = 0 \tag{47}$$

Region-3:

$$\frac{d^2u_3}{dy^2} = P \tag{48}$$

$$\frac{d^2\theta_3}{dy^2} + Ec\,\Pr\left(\frac{du_3}{dy}\right)^2 = 0 \tag{49}$$

The corresponding non-dimensional form of velocity boundary and interface conditions are

$$\begin{gathered} u_3 = 0 \quad \text{at} \quad y = -1,\; u_1 = 0 \quad \text{at} \quad y = 2, \\ u_2(0) = u_3(0),\;\; u_1(1) = u_2(1), \\ \frac{1}{m}\frac{du_2}{dy} = \frac{du_3}{dy} \;\text{ at }\; y = 0,\; \frac{du_1}{dy} = \frac{1}{m}\frac{du_2}{dy} \;\text{ at }\; y = 1 \end{gathered} \tag{50}$$

and the non-dimensional form of temperature boundary and interface conditions are

$$\begin{gathered} \theta_3 = 0 \quad \text{at} \quad y = -1,\; \theta_1 = 1 \quad \text{at} \quad y = 2, \\ \theta_2(0) = \theta_3(0),\;\; \theta_1(1) = \theta_2(1), \\ \frac{d\theta_2}{dy} = Cr\frac{d\theta_3}{dy} \;\text{ at }\; y = 0,\; \frac{d\theta_1}{dy} = \frac{1}{Cr}\frac{d\theta_2}{dy} \;\text{ at }\; y = 1 \end{gathered} \tag{51}$$

From the Eqs. (44)–(49) using (50) and (51) the exact solutions are

Region-1:

$$u_1 = \frac{P}{2}y^2 - P(2+y) \tag{52}$$

$$\theta_1 = l_1y^4 + l_2y^3 + l_3y^2 + D_7y + D_8 \tag{53}$$

Region-2:

$$u_2 = \frac{mP}{2}y^2 - P(2+my) \tag{54}$$

$$\theta_2 = l_4y^4 + l_5y^3 + l_6y^2 + D_9y + D_{10} \tag{55}$$

Region-3:

$$u_3 = \frac{P}{2}y^2 - P\left(2+y\right) \tag{56}$$

$$\theta_3 = l_7 y^4 + l_8 y^3 + l_9 y^2 + D_{11} y + D_{12} \tag{57}$$

The results of Eqs. (52)–(57) are compared with the results of Eqs. (44) – (49) using (50) and (51) which are obtained by using DTM.

Case-2: Absence Of Viscous Dissipation For Newtonian Fluid

For a Newtonian fluid $\left(K=0\right)$ in the absence of viscous dissipation $\left(Ec=0\right)$, $m=1$ and $Cr=1$ the non-dimensional equations become

$$\frac{d^2u_i}{dy^2} = P \tag{58}$$

$$\frac{d^2\theta_i}{dy^2} = 0 \tag{59}$$

for $i = 1, 2, 3$.

The corresponding boundary and interface conditions for velocity and temperature are

$$\begin{gathered} u_3 = 0 \quad \text{at} \quad y=-1, \; u_1 = 0 \quad \text{at} \quad y=2, \\ u_2\left(0\right) = u_3\left(0\right), u_1\left(1\right) = u_2\left(1\right), \\ \frac{du_2}{dy} = \frac{du_3}{dy} \text{ at } y=0, \frac{du_1}{dy} = \frac{du_2}{dy} \text{ at } y=1, \end{gathered} \tag{60}$$

$$\begin{gathered} \theta_3 = 0 \quad \text{at} \quad y=-1, \; \theta_1 = 1 \quad \text{at} \quad y=2, \\ \theta_2(0) = \theta_3(0), \; \theta_1(1) = \theta_2(1), \\ \frac{d\theta_2}{dy} = \frac{d\theta_3}{dy} \text{ at } y=0, \frac{d\theta_1}{dy} = \frac{d\theta_2}{dy} \text{ at } y=1 \end{gathered} \tag{61}$$

The exact solutions of Eqs. (58) and (59) using (60) and (61) are

$$u_i = \frac{P}{2}y\left(y-1\right) - P \tag{62}$$

$$\theta_i = \frac{y+1}{3} \tag{63}$$

The results of Eqs. (62) and (63) are compared with the results of Eqs. (58) and (59) using (60) and (61) which are obtained by using DTM.

4. DETERMINATION OF HEAT TRANSFER, SKIN FRICTION, AND MASS FLOW RATE

Apart from the velocity and temperature distribution in the channel, it is important to determine the physical quantities such as the rate of heat transfer, the skin friction, and the mass flow rate.

4.1. Rate of Heat Transfer

Knowing the temperature distribution one can determine the rate of heat transfer through the channel wall to the fluid which is given by

$$q_B = \left(\frac{d\theta_3}{dy}\right)_{y=-1} \text{ and } q_T = \left(\frac{d\theta_1}{dy}\right)_{y=2} \tag{64}$$

The rate of heat transfer at the top and bottom wall is given by

$$\begin{aligned} q_T &= \left(b_3 + 2ab_4 + ab_6\right)\cosh\left(2a\right) + \left(2ab_3 + b_4 + ab_5\right)\sinh\left(2a\right) + 2ab_1 \sinh\left(4a\right) \\ &\quad + 2ab_2 \cosh\left(4a\right) + 32b_7 + 12b_8 + 4b_9 + C_1 \\ q_B &= \left(b_{15} - ab_{16} + ab_{18}\right)\cosh\left(a\right) + \left(ab_{15} - b_{16} - ab_{17}\right)\sinh\left(a\right) + 2ab_{14} \cosh\left(2a\right) \\ &\quad - 2ab_{13} \sinh\left(2a\right) - 4b_{19} + 3b_{20} - 2b_{21} + C_5 \end{aligned}$$

4.2. Skin Friction

The skin frictions at the top and bottom plates τ_T and τ_B are given in non-dimensional form by

$$\tau_B = \left(\frac{du}{dy}\right)_{y=-1} \text{ and } \tau_T = \left(\frac{du_1}{dy}\right)_{y=2} \tag{65}$$

$$\begin{aligned} \tau_T &= \left(1+K\right)\left(al_1 \sinh\left(2a\right) + al_2 \cosh\left(2a\right) + 4l_3 + d_9\right) + K\left(d_1 \cosh\left(2a\right) + d_2 \sinh\left(2a\right)\right) \\ &\quad - \frac{2PK}{K+2} - A\left(\frac{K+1}{K+2}\right) \end{aligned}$$

$$\tau_B = \left(1+K\right)\left(al_5 \cosh\left(a\right) - al_4 \sinh\left(a\right) - 2l_3 + d_9\right)$$

4.3. Mass Flow Rate

Keeping in view the physical importance, the mass flow rate through the channel is computed and is given by

$$M = \int_{-1}^{2} u dy = \frac{l_5}{a} - \frac{d_9}{2} + d_{10} + \frac{mP}{6} + \frac{d_5}{2} + d_6 + \frac{8l_3}{3} + \frac{3d_3}{2} + d_4 + \frac{(l_4 - l_1)}{a}\sinh(a) - \frac{(l_5 + l_2)}{a}\cosh(a) + \frac{l_1}{a}\sinh(2a) + \frac{l_2}{a}\cosh(2a) \tag{66}$$

5. Results and Discussion

An exact analytical solution for the viscous fluid sandwiched between two micropolar fluid layers is studied. The basic differential equations governing the flow are linear coupled ordinary differential equations and hence exact solutions are found. The solutions are also obtained using Differential Transform Method (DTM). The direct solutions and DTM solutions agree very well. Though exact solutions can be obtained for the governing equations, the solutions are also found using DTM due to the reason that the computational procedure in finding the direct solutions is highly tedious whereas the same solutions can be obtained using DTM with less computation. Further using DTM one can solve the solutions of even nonlinear coupled differential equations.

The effect of the material parameter K on the velocity profiles is shown in Figure 2. It is seen that as K increases, the velocity decreases in all the three regions. However the maximal velocity is obtained in region – 2 which is a viscous fluid layer. It is interesting to observe that the effect of material parameter K is also effective in viscous fluid layer, this is due to the coupling effect. The effect of material parameter K is similar to the result obtained by Umavathi et al. [20].

Figure 3 displays the effect of material parameter K on the microrotation velocity N. We notice that as K increases microrotation velocity increases in magnitude for values of $K = 0.01$, 0.1, 0.5 and 1.0 in region-1 and 3 (micropolar fluid) and remain invariant in region–2 (viscous fluid). This is an excepted result because an increase in material parameter implies an increase in the spin gradient viscosity which promotes the rotational velocity.

The effect of viscosity ratio m which is taken as the ratio of viscosity of the micropolar fluid to viscosity of the viscous fluid $m(=\mu_1/\mu)$ on the velocity field is shown in Figure 4. As the viscosity ratio m increases the velocity also increases, but the magnitude of promotion is large for viscous fluid layer $(K = 0)$ when compared to the micropolar fluid layer $(K = 0)$. There is no effect of viscosity ratio m on the microrotation velocity. This is due to the fact that the viscosity ratio m do not occur in the governing equations for the microrotation velocity.

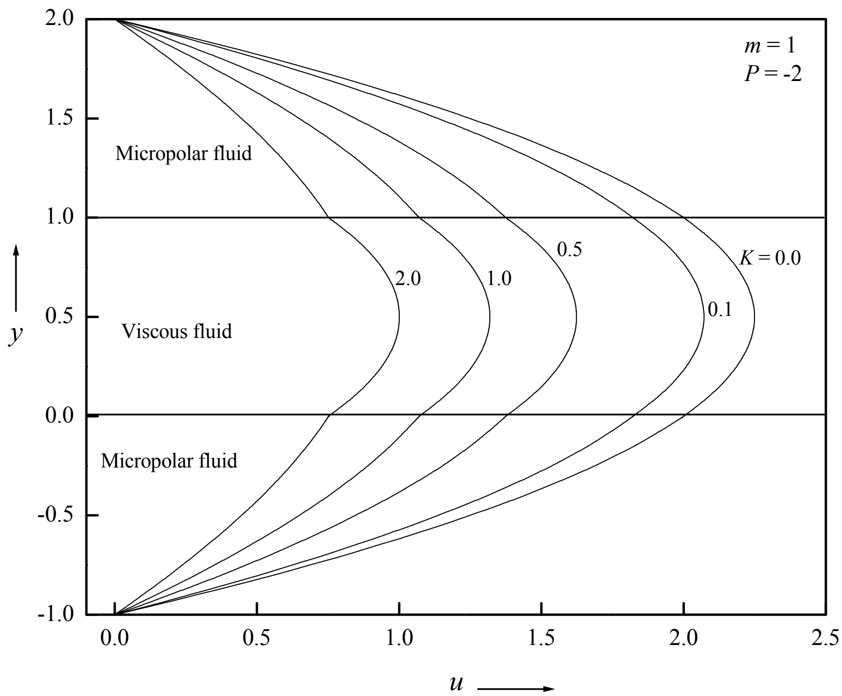

Figure 2. Velocity profiles for different values of material parameter K .

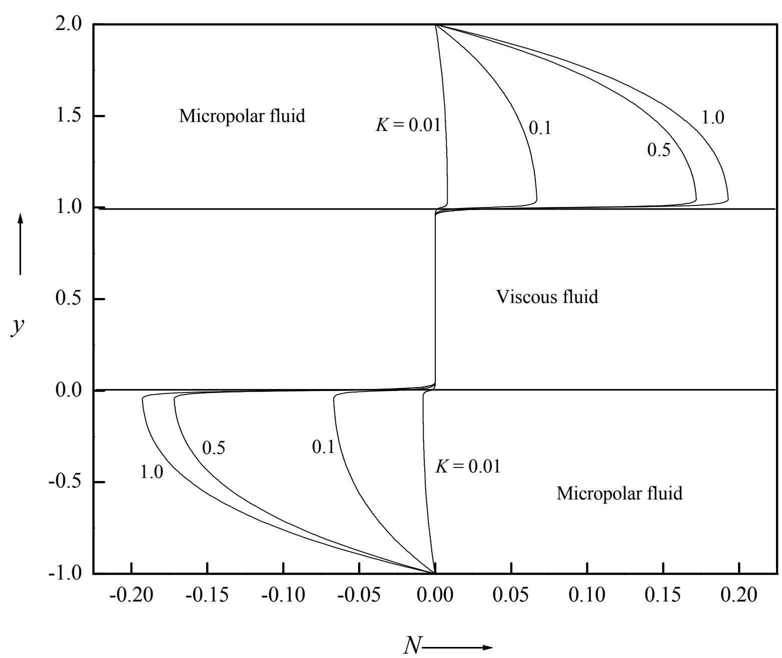

Figure 3. Microrotation velocity profiles for different values of material parameter K .

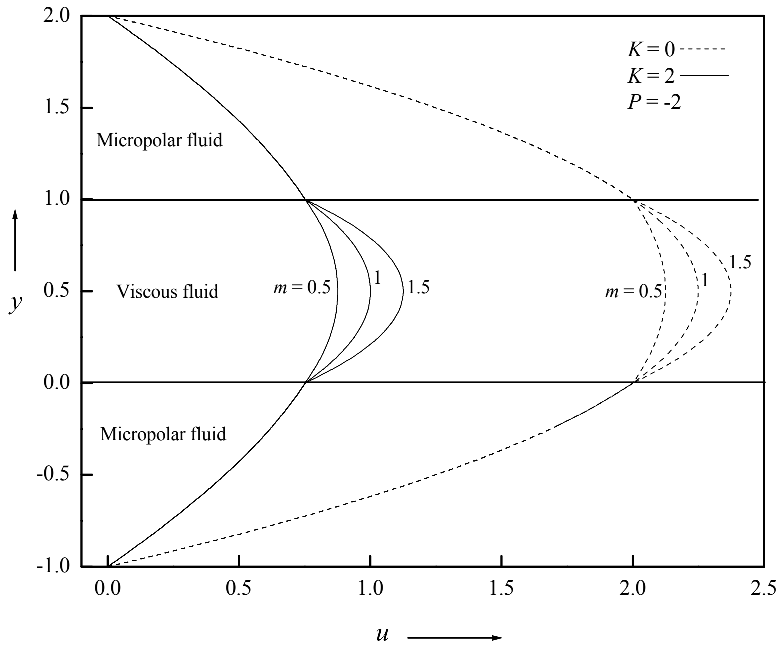

Figure 4. Velocity profiles for different values of material parameter K and viscosity ratio m .

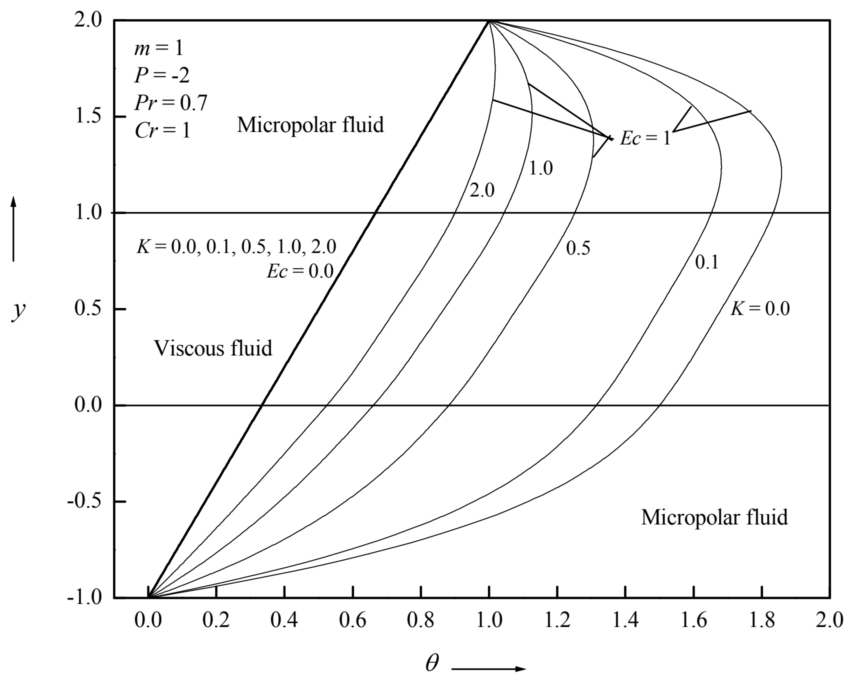

Figure 5. Temperature profiles for different values of material parameter K .

Figure 5 displays the effect of material parameter K on the temperature profiles in the presence and in the absence of viscous dissipation. In the presence of viscous dissipation $(Ec = 1)$, the effect of material parameter K decreases the temperature field in all the three regions. Here also the maximal temperature is observed for Newtonian fluid when compared to micropolar fluid in the presence of viscous dissipation. It is seen from the basic equations that in the absence of viscous dissipation $(Ec = 0)$ the temperature profiles become linear and do not depend on either the velocity or the microrotation velocity. Therefore we observe a linear profile which is a straight line for both Newtonian and micropolar fluid in the absence of viscous dissipation.

The effect of viscosity ratio m on the temperature field is shown in Figure 6. As the viscosity ratio m increases the temperature increases in all the three regions for both Newtonian $(K = 0)$ and micropolar fluid $(K = 2)$. Here also the magnitude of temperature profiles is large for viscous fluid when compared to micropolar fluid in the presence of viscous dissipation. The temperature profile is linear in the absence of viscous dissipation and hence do not vary for different values of viscosity ratio.

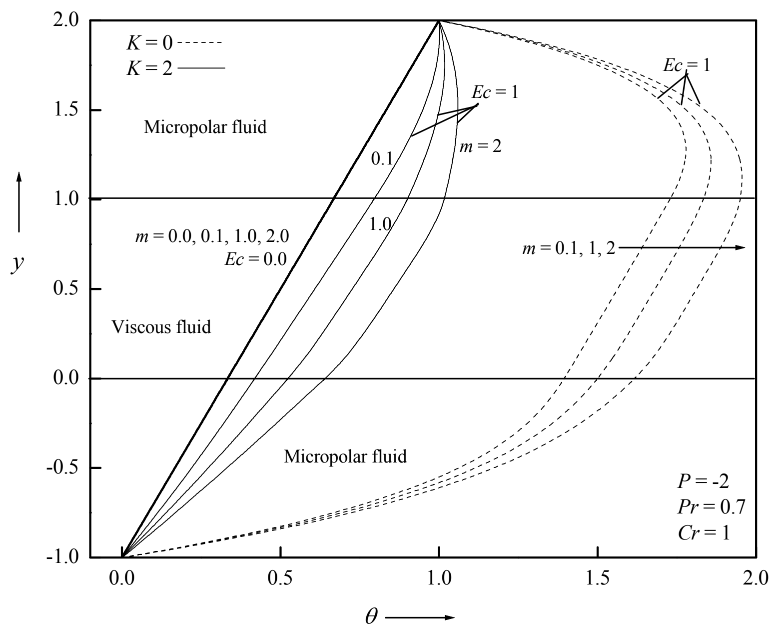

Figure 6. Temperature profiles for different values of material parameter K and viscosity ratio m.

Figure 7 shows the effect of the conductivity ratio Cr on the temperature field. It seen that as the conductivity ratio increases, the temperature increases in the upper half of the region–2 and decreases in the lower half of the region–2 which is the similar result obtained by Umavathi et al. [20]. It is also seen that the value of the temperature for different values of the conductivity ratio remains the same at the middle of the channel ($y = 0.5$) for both Newtonian and micropolar fluids. Here also in the absence of viscous dissipation the temperature profile is linear and do not vary for different values of conductivity ratio.

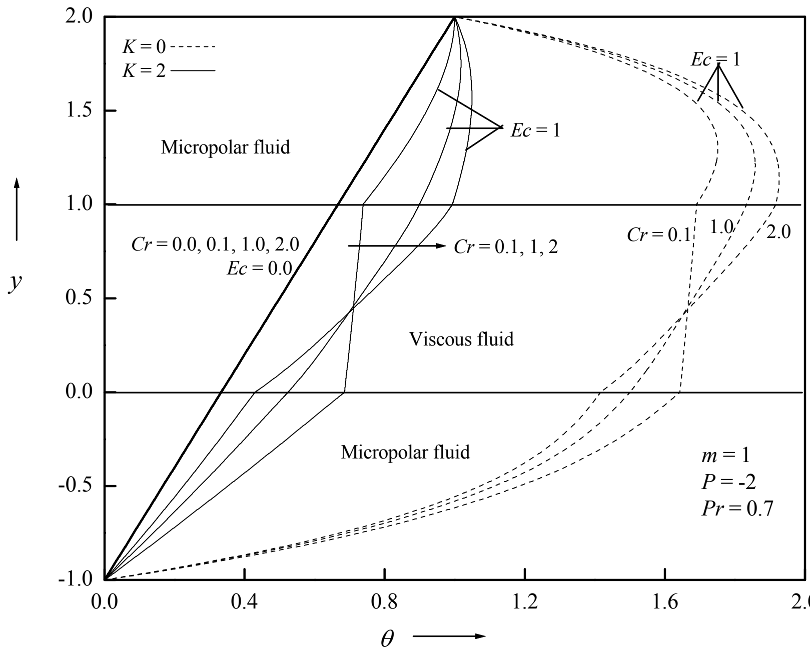

Figure 7. Temperature profiles for different values of material parameter K and conductivity ratio Cr .

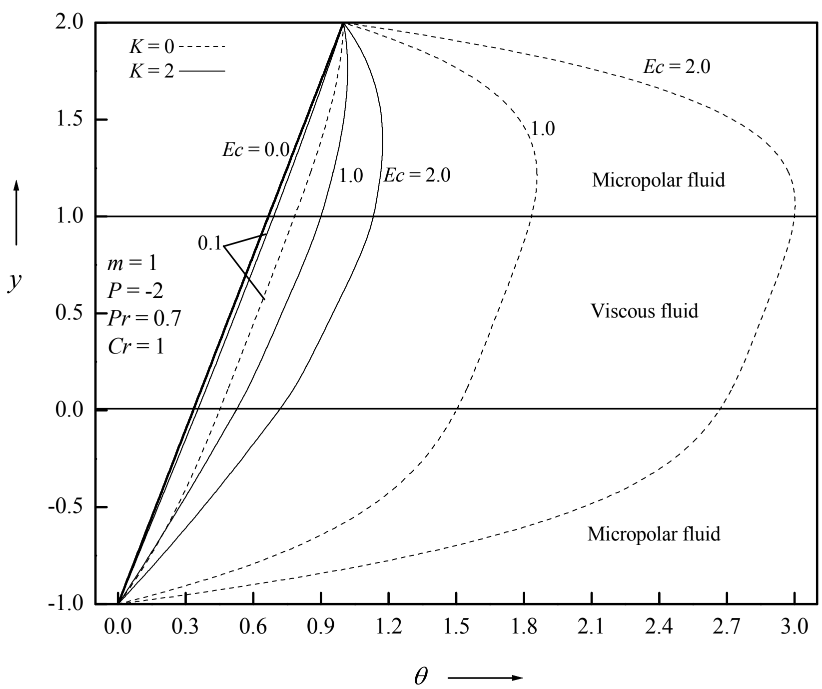

Figure 8. Temperature profiles for different values of material parameter K and Eckert number Ec .

Figures 8 and 9 show the effect of Eckert number and Prandtl number on the temperature filed. It is seen that as the Eckert number and Prandtl number increases the temperature increases for both Newtonian and micropolar fluids. Here also the magnitude is large for Newtonian fluid compared to the micropolar fluid. In the absence of viscous dissipation the temperature profile is linear and is not affected by the Eckert number and Prandtl number for both Newtonian and micropolar fluids.

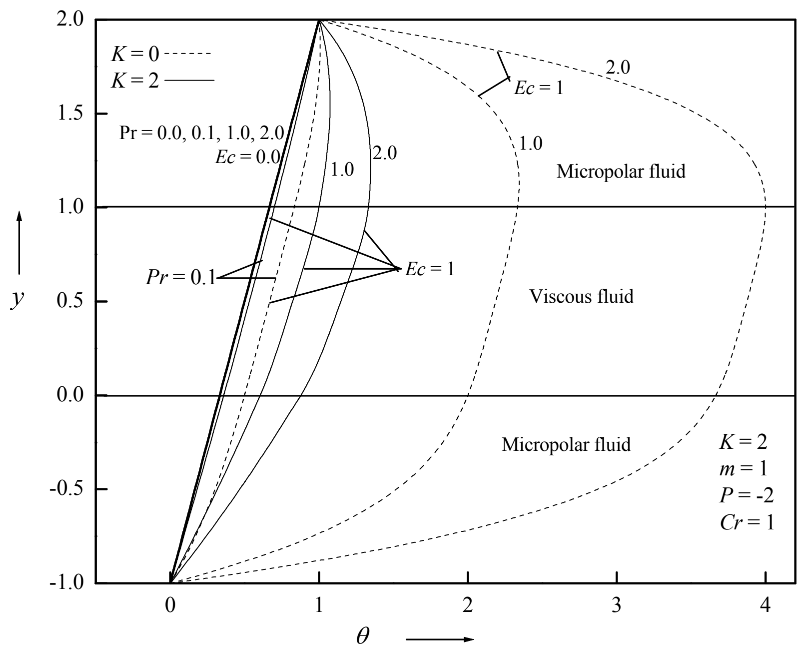

Figure 9. Temperature profiles for different values of material parameter K and Prandtl number $\Pr$.

Because of the importance of the viscosity, the shear viscosity μ_1 of a micropolar fluid on the velocity and microrotation velocities for 20% and 40% RBC (Red blood corpuscles) concentration has been computed and is shown graphically in Figs. 10 and 12 for different values of μ_R. In the present analysis the shear viscosity μ_1 of the micropolar fluid is taken in the form μ_R/K where μ_R is cell rotational viscosity (the values of μ_R are taken from Ariman et al. [10]). The present results can be obtained from Ariman et al. [10] replacing μ_1 by μ and μ_R by μK in cylindrical polar co-ordinates.

Figures 10 and 11 shows the effect of the shear viscosity μ_R on the velocity and the temperature fields for $K = 1$ and $K = 2$. We notice that velocity and temperature increases as μ_R increases. However its effect on the vecoity field is significant in the viscous region and is almost invariant in the micropolar fluid region. It is also observed that the velocity and temperature fields are invariant on μ_R for Glycerin. This is because the viscosity of Glycerin is high and hence the viscosity of the suspended particles will be negligible.

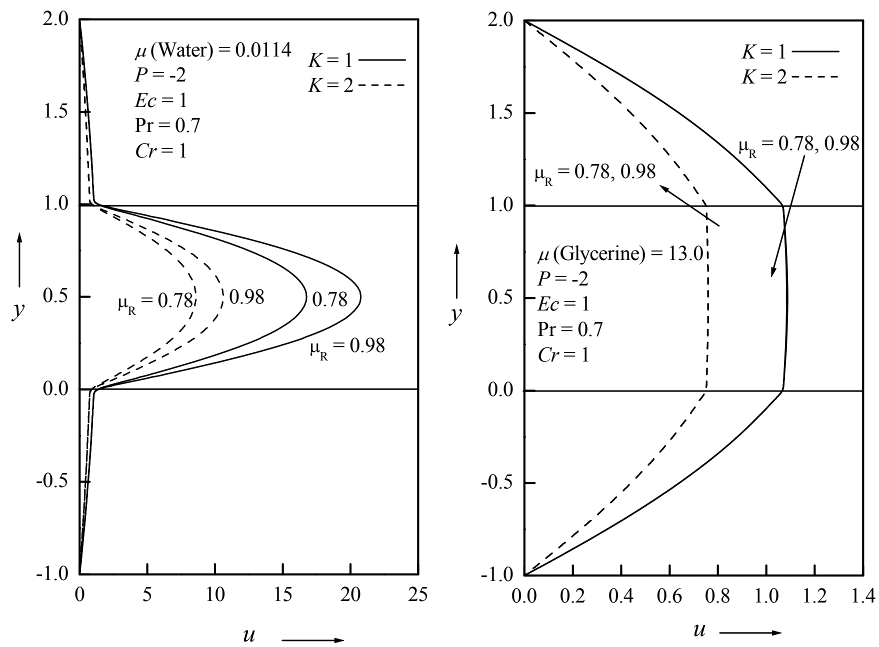

Figure 10. Velocity profiles for different values of effective viscosity.

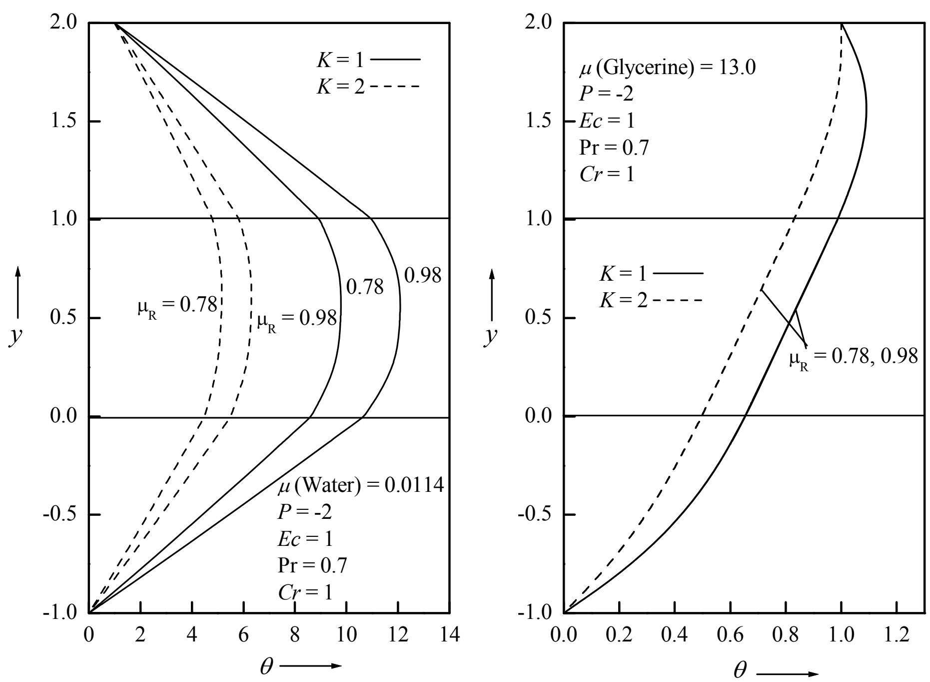

Figure 11. Temperature profiles for different values of effective viscosity.

Table 2 shows the results obtained by differential transform method and by direct method. Excellent agreement is found between these two methods in the presence and in the absence of viscous dissipation. Therefore differential transform method is the best method which will minimize not only computation but also can be applied for nonlinear equations for which direct solutions can not be obtained.

Table 2. Comparison of DTM solution with direct solution

For micropolar fluid with $m=1$, $K=2$, $Cr=1$, $Ec=0.5$, $\Pr=0.7$.						
	Velocity		Micro-rotation velocity		Temperature	
y	DTM	Exact	DTM	Exact	DTM	Exact
2.00	0	0	0	0	1.0000000	1.0000000
1.50	0.4462278	0.4462278	0.1477356	0.1477356	1.0225043	1.0225043
1.00	0.7518910	0.7518910	0.1747515	0.1747515	0.9419750	0.9419750
1.00	0.7518910	0.7518910	0	0	0.9419750	0.9419750
0.50	1.0018910	1.0018910	0	0	0.7898916	0.7898916
0	0.7518910	0.7518910	0	0	0.6086416	0.6086416
0	0.7518910	0.7518910	-0.1747515	-0.1747515	0.6086416	0.6086416
-0.50	0.4462278	0.4462278	-0.1477356	-0.1477356	0.3558376	0.3558376
-1.00	0	0	0	0	0	0
	For Newtonian fluid with $m=1$, $K=0$, $Cr=1$, $Ec=0.5$, $\Pr=0.7$.					
2.00	0	0	0	0	1.00000	1.00000
1.50	1.25000	1.25000	0	0	1.30729	1.30729
1.00	2.00000	2.00000	0	0	1.25000	1.25000
1.00	2.00000	2.00000	0	0	1.25000	1.25000
0.50	2.25000	2.25000	0	0	1.09062	1.09062
0	2.00000	2.00000	0	0	0.91667	0.91667
0	2.00000	2.00000	0	0	0.91667	0.91667
-0.50	1.25000	1.25000	0	0	0.64063	0.64063
-1.00	0	0	0	0	0	0
	For Newtonian fluid in the absence of viscous dissipation with $m=1$, $K=0$, $Cr=1$, $Ec=0$, $\Pr=0.7$.					
2.00	0	0	0	0	1.00000	1.00000
1.50	1.25000	1.25000	0	0	0.83333	0.83333
1.00	2.00000	2.00000	0	0	0.66667	0.66667
1.00	2.00000	2.00000	0	0	0.66667	0.66667
0.50	2.25000	2.25000	0	0	0.50000	0.50000
0	2.00000	2.00000	0	0	0.33333	0.33333
0	2.00000	2.00000	0	0	0.33333	0.33333
-0.50	1.25000	1.25000	0	0	0.16667	0.16667
-1.00	0	0	0	0	0	0

Owing to the practical applications, the variation of viscosity ratio, material parameter, conductivity ratio, Eckert number and Prandtl number on the rate of heat transfer, skin friction and mass flow rate are tabulated in Table 3.

Table 3. The rate of heat transfer, the skin friction at the top and bottom plates, and the mass flow rate for different values of m, K, Cr, Ec and Pr

		q_T	q_B	τ_T	τ_B	M
m	0.5	-0.139124	0.805791	-1.0000	1.0000	1.68042
	1.0	-0.197458	0.864124	-1.0000	1.0000	1.76376
	1.5	-0.255791	0.922458	-1.0000	1.0000	1.84709
	2.0	-0.314124	0.980791	-1.0000	1.0000	1.93042
K	0.0	-2.81667	3.48333	-3.0000	3.0000	4.5
	0.1	-2.29991	2.96658	-2.7273	2.7273	4.11366
	0.5	-1.20118	1.86784	-2.0000	2.0000	3.12876
	1.0	-0.632965	1.29963	-1.5000	1.5000	2.45812
	2.0	-0.197458	0.864124	-1.0000	1.0000	1.76376
Cr	0.1	-0.0546007	1.00698	-1.0000	1.0000	1.76376
	0.5	-0.130791	0.930791	-1.0000	1.0000	1.76376
	1.0	-0.197458	0.864124	-1.0000	1.0000	1.76376
	2.0	-0.280791	0.780791	-1.0000	1.0000	1.76376
Ec	0.1	0.280254	0.386412	-1.0000	1.0000	1.76376
	0.5	0.0679378	0.598729	-1.0000	1.0000	1.76376
	1.0	-0.197458	0.864124	-1.0000	1.0000	1.76376
	2.0	-0.728249	1.39492	-1.0000	1.0000	1.76376
Pr	0.1	0.257506	0.409161	-1.0000	1.0000	1.76376
	0.5	-0.0458032	0.71247	-1.0000	1.0000	1.76376
	1.0	-0.197458	0.864124	-1.0000	1.0000	1.76376
	2.0	-1.18321	1.84988	-1.0000	1.0000	1.76376

As the viscosity ratio m increases the rate of heat transfer decreases at the top plate and increases at the bottom plate. The skin friction remains invariant for variation of viscosity ratio whereas mass flow rate increases as the viscosity ratio increases. The rate of heat transfer and skin friction decreases in magnitude at both the plates as the material parameter K increases. The mass flow rate also decreases as K increases. The conductivity ratio decreases the rate of heat transfer at both the plates.

The effect of increasing the Eckert number and Prandtl number decreases the rate of heat transfer at the top plate and increases at the bottom plate. The skin friction and mass flow rate are not affected for variation of conductivity ratio, Eckert number and Prandtl number which is the similar result observed by Umavathi et al. [20].

CONCLUSION

The fully developed viscous fluid sandwiched between micropolar fluids was analyzed by integrating the equations and by differential transform method. It was found that the effect of material parameter suppresses the velocity and temperature field whereas it promotes the microrotation velocity. The viscosity ratio was to promote the flow. The conductivity ratio was to suppress the temperature field at lower plate and promote at the upper plate. The Eckert number and Prandtl number promotes the temperature field. The rate of heat transfer decreases at the top plate and increases at the bottom plate for variations of viscosity ratio, material parameter, conductivity ratio, Eckert number and Prandtl number. The mass flow rate decreases as the viscosity ratio and material parameter increases whereas it is not affected for variations of conductivity ratio, Eckert number and Prandtl number. The effect of cell rotational viscosity is to increase the velocity for water and is invarient for Glycerin. It was also observed that the profiles for Newtonian fluid are maximal when compared to micropolar fluid. Differential transform method and the direct method was found to be in good agreement.

REFERENCES

[1] A. C. Eringen. Theory of micropolar continua. In: Proceedings of the Ninth Midwestern Mechanics Conference, 1965, pp. 23.

[2] A. C. Eringen, Simple microfluids, *Int. J. Eng. Sci.* 2 (1964) 205–217.

[3] A. C. Eringen, Theory of micropolar fluids, *J. Math. Mech*. 16 (1966) 1–18.

[4] M. M. Khonsari, D. Brew, On the performance of finite journal bearing lubricated with micropolar fluids, *ASLE Tribology Trans*. 32 (1989) 155–160.

[5] M. M. Khonsari, On the self-excited whirl orbits of a journal in a sleeve bearing lubricated with micropolar fluids, *Acta Mech*. 81(1990) 235–244.

[6] B. Hadimoto, T. Tokioka, Two-dimensional shear flows of linear micropolar fluids, *Int. J. Eng. Sci*. 7 (1969) 515–522.

[7] J. D. Lee, A.C. Eringen, Boundary effects of orientation of nematic liquid crystals, *J. Chem. Phys*. 55 (1971) 4509–4512.

[8] F. Lockwood, M. Benchaitra, S. Friberg, Study of polyotropic liquid crystals in viscometric flow and clastohydrodynamic contact, *ASLE Tribology Trans*. 30 (1987) 539–548.

[9] T. Ariman, M.A. Turk, N.D. Sylvester, Microcontinuum fluid mechanics–a review, *Int. J. Eng. Sci*. 11 (1973) 905–930.

[10] T. Ariman, M.A. Turk, N.D. Sylvester, Application of microcontinum fluid mechanics, *Int. J. Eng. Sci*. 12 (1974) 273–293.

[11] G. Lukaszewicz, *Micropolar Fluids: Theory and Application*, Birkhäuser, Basel, 1999.

[12] A. C. Eringen, *Microcontinum Field Theories, II: Fluent Media*, Springer, New York, 2001.

[13] J. C. Umavathi, Jaweriya Sultana, Mixed convection of a micropolar fluid in a vertical channel with boundary conditions of third kind, *Int. J. Engng. Sci. Tech*. 3(4) (2011) 213-224.

[14] M. M. Rashidi, S.A. Mohimanian Pour, S. Abbasbandy, Analytic approximate solutions for heat transfer of a micropolar fluid through a porous medium with radiation, *Commun. Nonlinear Sci. Numer. Simulat*. 16 (2011) 1874–1889.

[15] Md. Ziaul Haque, Md. Mahmud Alam, M. Ferdows, A. Postelnicu, Micropolar fluid behaviors on steady MHD free convection and mass transfer flow with constant heat and mass fluxes, joule heating and viscous dissipation, *J. King Saud University – Eng. Sci*. 24 (2012) 71–84.

[16] S.I. Bakhtiyarov, D.A. Siginer. *A note on the laminar coreannular flow of two immiscible fluids in a horizontal tube. In: Proceedings of international symposium on*

liquid–liquid two phase flow and transport phenomena, Begell house, Inc., Santa Barbara, 1997, pp 107–111.

[17] A. J. Chamkha, Oscillatory flow and heat transfer in two immiscible fluids, *Int. J. Fluid Mech*. Res. 31 (2004) 13–36.

[18] A. J. Chamkha, Flow of two-immiscible fluids in porous and nonporous channels, *J. Fluids Eng*. 122 (2000) 117–124.

[19] J. C. Umavathi, A.J. Chamkha, M.H. Manjula, A. Al-Mudhaf. Flow and heat transfer of a couple stress fluid sandwiched between viscous fluid layers, *Can. J. Phys*. 83 (2005) 705-720.

[20] J. C. Umavathi, J. Prathap Kumar, A.J. Chamkha, Flow and heat transfer of a couple-stress fluid sandwiched between viscous fluid layers, *Can. J. Phys*. 86 (2008) 961–973.

[21] Md. A. Ikbal, S. Chakravarty, P.K. Mandal, Two-layered micropolar fluid flow through stenosed artery: Effect of peripheral layer thickness, *Comp. Math. Appl*. 58 (2009) 1328-1339.

[22] J. C. Umavathi, M. Shekar, Mixed convective flow of two immiscible viscous fluids in a vertical wavy channel with traveling thermal waves, *Heat Transfer Asian Research* 40(8) (2011) 721-743.

[23] J. C. Umavathi, I.C. Liu, M. Shekar, Unsteady mixed convective heat transfer of two immiscible fluids confined between a long vertical wavy wall and a parallel flat wall, *Appl. Math. Mech*. 33(7) (2012a) 931–950.

[24] J. C. Umavathi, J. Prathap Kumar, M. Shekar, Convective flow between a corrugated and a smooth wall, *J. Porous Media*, 15(10) (2012b) 975-988.

[25] J. C. Umavathi, I.C. Liu, J. Prathap-Kumar, D. Shaik-Meera, Unsteady flow and heat transfer of porous media sandwiched between viscous fluids, *Appl. Math, Mech*. 31 (2010) 1497-1516.

[26] M. S. Malashetty J.C. Umavathi, J. Prathap Kumar, Flow and heat transfer in an inclined channel containing a fluid layer sandwiched between two porous layers, *J. Porous Media* 8(5) (2005) 443-453.

[27] M. S. Malashetty, J.C. Umavathi, J. Prathap Kumar, Magnetoconvection of two-immiscible fluids in a vertical enclosure, *Heat Mass Transfer*, 42(11) (2006) 977-993.

[28] J. Prathap Kumar, J.C. Umavathi, Ali J. Chamkha, Ioan Pop, Fully-developed free-convective flow of micropolar and viscous fluids in a vertical channel, *Appl. Math. Modelling* 34 (2010) 1175–1186.

[29] K. Zhou, *Differential transformation and its applications for electrical circuits*, Huazhong Univ. Press; 1986. (in Chinese)

[30] C. K. Chen, S.H. Ho, Solving partial differential equations by two dimensional differential transform method, *Appl. Math. Comput*. 106 (1999) 171–179.

[31] F. Ayaz, Solutions of the systems of differential equations by differential transform method, *Appl. Math. Comput*. 147 (2004) 547–567.

[32] I. H. Abdel-Halim Hassan, Comparison differential transformation technique with Adomian decomposition method for linear and nonlinear initial value problems, *Chaos, Solitons and Fractals* 36 (2008) 53–65.

[33] A. S. V. Ravi Kanth, K. Aruna, Solution of singular two-point boundary value problems using differential transformation method, *Physics Letters A* 372 (2008) 4671–4673.

[34] D. D. Ganji, H. Bararnia, S. Soleimani, E. Ghasemi, Analytical solution of the magneto-hydrodynamic flow over a nonlinear stretching sheet, *Modern Physics Lett. B* 23 (2009) 2541–2556.

[35] A. A. Joneidi, D.D. Ganji, M. Babaelahi, Differential transformation method to determine fin efficiency of convective straight fins with temperature dependent thermal conductivity, *Int. Commun. Heat Mass Transf*. 36 (2009) 757–762.

[36] M. M Rashidi, The modified differential transform method for solving MHD boundary-layer equations, *Comp. Phys. Commun*. 180 (2009) 2210–2217.

[37] M. M. Rashidi, S.A. Mohimanian Pour, A novel analytical solution of heat transfer of a micropolar fluid through a porous medium with radiation by DTM-Padé, *Heat Transfer—Asian Research*, 39(8) (2010) 575-589.

[38] M. J. Jang, Y.L. Yeh, C.L. Chen, W.C. Yeh, Differential transformation approach to thermal conductive problems with discontinuous boundary condition, *Appl. Math. Compu*. 216 (2010) 2339–2350.

[39] M. Keimanesha, M.M. Rashidi, Ali J. Chamkha, R. Jafari, Study of a third grade non-Newtonian fluid flow between two parallel plates using the multi-step differential transform method, *Comp. Math. Appl*. 62 (2011) 2871–2891.

[40] H. Yaghoobi, M. Torabi, The application of differential transformation method to nonlinear equations arising in heat transfer, *Int. Comm. Heat and Mass Transfer* 38 (2011) 815–820.

[41] D. A. S. Rees, A.P. Bassom. The Blasius boundary-layer flow of a micropolar fluid, *Int. J. Eng. Sci*. 34, 113 (1996).